Article:
Edmans, J.G., Ollington, B., Colley, H.E. et al. (2022) Electrospun patch delivery of anti-TNFα F(ab) for the treatment of inflammatory oral mucosal disease. Journal of Controlled Release, 350. pp. 146-157. ISSN: 0168-3659

https://doi.org/10.1016/j.jconrel.2022.08.016

Journal of Controlled Release 350 (2022) 146–157

Contents lists available at ScienceDirect

Journal of Controlled Release

journal homepage: www.elsevier.com/locate/jconrel

Electrospun patch delivery of anti-TNFα F(ab) for the treatment of inflammatory oral mucosal disease

Jake G. Edmans [a,b], Bethany Ollington [a], Helen E. Colley [a,*], Martin E. Santocildes-Romero [c], Lars Siim Madsen [c], Paul V. Hatton [a], Sebastian G. Spain [b], Craig Murdoch [a]

[a] School of Clinical Dentistry, 19 Claremont Crescent, University of Sheffield, Sheffield S10 2TA, UK
[b] Department of Chemistry, Brook Hill, University of Sheffield, Sheffield S3 7HF, UK
[c] AFYX Therapeutics, Lergravsej 57, 2. tv, 2300 Copenhagen, Denmark

ARTICLE INFO

Keywords:
Electrospinning
Drug delivery
Antibodies
Oral medicine
Oral patches
TNFα

ABSTRACT

Chronic ulcerative oral mucosal inflammatory diseases, including oral lichen planus and recurrent aphthous stomatitis, are painful and highly prevalent, yet lack effective clinical management. In recent years, systemic biologic therapies, including monoclonal antibodies that block the activity of cytokines, have been increasingly used to treat a range of immune-mediated inflammatory conditions such as rheumatoid arthritis and psoriasis. The ability to deliver similar therapeutic agents locally to the oral epithelium could radically alter treatment options for oral mucosal inflammatory diseases, where pro-inflammatory cytokines, in particular tumour-necrosis factor-α (TNFα), are major drivers of pathogenesis.

To address this, an electrospun dual-layer mucoadhesive patch comprising medical-grade polymers was investigated for the delivery of F(ab) biologics to the oral mucosa. A fluorescent-labelled F(ab) was incorporated into mucoadhesive membranes using electrospinning with 97% *v*/v ethanol as a solvent. The F(ab) was detected within the fibres in aggregates when visualised by confocal microscopy. Biotinylated F(ab) was rapidly eluted from the patch (97 ± 5% released within 3 h) without loss of antigen-binding activity. Patches applied to oral epithelium models successfully delivered the F(ab), with fluorescent F(ab) observed within the tissue and 5.1 ± 1.5% cumulative transepithelial permeation reached after 9 h. Neutralising anti-TNFα F(ab) fragments were generated from whole IgG by papain cleavage, as confirmed by SDS-PAGE, then incorporated into patches. F(ab)-containing patches had TNFα neutralising activity, as shown by the suppression of TNFα-mediated CXCL8 release from oral keratinocytes cultured as monolayers. Patches were applied to lipopolysaccharide-stimulated immune-competent oral mucosal ulcer equivalents that contained primary macrophages. Anti-TNFα patch treatment led to reduced levels of active TNFα along with a reduction in the levels of disease-implicated T-cell chemokines (CCL3, CCL5, and CXCL10) to baseline concentrations. This is the first report of an effective device for the delivery of antibody-based biologics to the oral mucosa, enabling the future development of new therapeutic strategies to treat painful conditions.

1. Introduction

Chronic ulcerative oral mucosal inflammatory diseases greatly affect quality of life. Oral lichen planus (OLP) and recurrent aphthous stomatitis (RAS) are the most prevalent causes of oral ulcers, affecting up to 25% of the population worldwide to some degree [1,2]. Although the early pathogenesis of these diseases is not fully understood, progression towards tissue ulceration is known to be mediated by tumour necrosis factor alpha (TNFα), a potent pro-inflammatory cytokine secreted by activated T-cells, macrophages and mast cells at lesional sites [3,4]. TNFα induces neighbouring oral keratinocytes and fibroblasts to release chemokines that recruit further lymphocytes and other immune cells. Ultimately, cytotoxic T-cells in the inflammatory infiltrate along with TNFα trigger apoptosis of the oral mucosal basal keratinocytes, leading to loss of the epithelium and ulcer formation.

OLP and RAS have no approved licenced treatments and symptoms are currently managed using topical corticosteroid ointments or oral rinses [1,5]. These are often unpleasant to use and their efficacy is in

* Corresponding author at: School of Clinical Dentistry, 19 Claremont Crescent, University of Sheffield, Sheffield S10 2TA, UK.
E-mail address: h.colley@sheffield.ac.uk (H.E. Colley).

https://doi.org/10.1016/j.jconrel.2022.08.016
Received 2 May 2022; Received in revised form 1 August 2022; Accepted 10 August 2022
Available online 18 August 2022

clinical practise impacted by low patient compliance [6]. In recent years, there has been considerable interest in neutralising monoclonal antibody therapy as an emerging treatment for oral mucosal inflammatory diseases, with particular attention being paid to anti-TNFα agents (for example infliximab, adalimumab, etanercept and certolizumab pegol), as these have been effective for other inflammatory conditions such as rheumatoid arthritis [7]. These biologics are considered to have a more targeted immunosuppressive effect in comparison to corticosteroids and have already shown efficacy when administered intravenously to patients with chronic oral ulcers [8,9]. However, systemic delivery requires high dosing and is associated with off-target toxicity [8]. Topical delivery of biologics directly to oral ulcers may circumvent these problems [10,11]. Indeed, topical dressings containing infliximab have been shown to be effective in treating chronic dermal ulcers [12]. Despite clinical interest, there has been no investigation to date into their efficacy when delivered topically to oral mucosal diseases.

Oromucosal delivery of biologics is hampered by the lack of suitable dosage forms that meet the requirement for their specific and efficient delivery to mucosal surfaces. Existing formulations such as oral rinses [13], gels [14] and tablets [15] deliver poorly defined doses of active ingredients uncontrollably throughout the oral cavity with short exposure times. To address this, we previously developed a mucoadhesive bilayer patch fabricated using electrospinning technology to promote unidirectional mucosal drug delivery [16,17]. We have previously shown that this oromucosal patch is highly effective at delivering small molecules such as the potent corticosteroid, clobetasol-17-propionate *in vitro* and in humans, where it has been successful at phase II clinical trials [18,19]. Moreover, the patch technology is particularly promising for the rapid release of biologically active proteins and peptides to oral mucosal surfaces [20], an application for which there are currently no alternative devices [17].

In this study we developed and evaluated a mucoadhesive electrospun patch for the delivery of anti-TNFα biologics directly to oral mucosal ulcers (Fig. S1). We show effective release of a biotinylated antibody fragment (F(ab)) from the patch with no loss of antigen binding functionality. Next, a patch was fabricated containing neutralising anti-TNFα F(ab) to act as a model therapeutic agent. Patch-eluted anti-TNFα F(ab) bound to TNFα and inhibited its pro-inflammatory actions by preventing TNFα-mediated release of CXCL8 from monolayer cultures of oral keratinocytes. Moreover, anti-TNFα patch treatment inhibited the actions of TNFα in a 3D tissue engineered immunocompetent *in vitro* model of an oral mucosal ulcer, leading to a reduction in immunogenic TNFα and TNFα-sensitive chemokine levels. This represents the first solid dosage form suitable for topical oromucosal biologic delivery and provides the first pre-clinical evidence in support of a novel treatment strategy that could radically affect the treatment of oral mucosal inflammatory diseases.

2. Material and methods

2.1. Materials

Unless otherwise indicated, all reagents used in enzyme-linked immunoassays (ELISA) were purchased from Bio-Techne (Abingdon, UK); all other reagents purchased from Sigma-Aldrich (Poole, UK). Poly (vinylpyrrolidone) (PVP; MW 2000 kDa) and Eudragit RS100 (RS100; MW 38 kDa) were kindly donated by BASF (Cheadle Hulme, UK) and Evonik Industries AG (Essen, Germany), respectively.

2.2. ELISA for the measurement of biotinylated F(ab) concentration

Biotinylated polyclonal goat anti-mouse F(ab) was used as a model protein to assess the suitability of the electrospun polymer system for the delivery of a biologically active antibody fragment. A direct ELISA protocol was developed to quantify the antigen binding activity of biotinylated anti-mouse antibodies and derivatives. High-binding 96-well plates were coated with IgG from mouse serum (10 μg/mL, 100 μL per well; Abcam, Cambridge, UK) overnight at room temperature and then blocked with BSA (1% *w/v*) overnight at 4 °C. Standards (78–5000 pg/mL; Abcam, Cambridge, UK) and samples containing biotinylated goat anti-mouse IgG F(ab) were loaded in duplicate and incubated for 2 h at room temperature before aspirating. Streptavidin-conjugated horseradish peroxidase (50 μg/mL) was added for 20 minutes before aspirating. Stabilised 3,3′,5,5′-tetramethylbenzidine/hydrogen peroxide substrate solution was added and incubated at room temperature followed 20 minutes later by aqueous hydrochloric acid (50 μL per well, 2 M) to stop the reaction. Plates were washed (0.05% *w/v* Tween 20 in PBS) 3 times after each aspiration step. Absorbance at 450 nm with a correction filter reading of 570 nm was measured using a spectrophotometer (Tecan, Männedorf, Switzerland) and concentrations interpolated from a standard curve fitted using the 4-parameter logistic curve setting in Graphpad Prism 9.3 software (GraphPad Software, La Jolla, USA).

2.3. Activity of biotinylated F(ab) after exposure to ethanol-water mixtures

Biotinylated goat anti-mouse F(ab) (1 μg/mL, 30 μL) was added to ethanol or different ratios of ethanol/water mixtures (970 μL) in glass vials. The solutions were incubated at room temperature for 1 h with shaking. Samples were then immediately diluted (1:100) in 1% *w/v* BSA and antigen-binding concentrations measured by ELISA. The measured antigen binding concentration was normalised against the known concentration to calculate percentage antigen-binding activity.

2.4. Electrospinning system and fabrication of mucoadhesive dual-layer patches

Electrospun membranes were fabricated using a system comprising a PHD2000 syringe pump (Harvard Apparatus, Cambridge, UK) and an Alpha IV Brandenburg power source (Brandenburg UK Ltd., Worthing, UK) as previously described [16]. Plastic syringes (1 mL volume; Henke Sass Wolf, Tuttlingen, Germany) were used to drive the solutions into a 20-gauge blunt metallic needle (Fisnar Europe, Glasgow, UK). Electrospinning was performed at room temperature with a potential difference of 19 kV, a flow rate of 2 mL/h, and a flight path of 14 cm. Mucoadhesive protein-containing membranes were electrospun as previously described from solutions containing PVP (10% *w/w*) and Eudragit RS100 (12.5% *w/w*) in 97% *v/v* ethanol [20]. The required amounts of PVP and RS100 were added to ethanol and mixed at room temperature using a magnetic stirrer until dissolved. F(ab) solutions were added, contributing to 3% *v/v* to the final solvent composition, and mixed briefly until homogeneous. Non-medicated (NM) patches were prepared by substituting the F(ab) solution with 3% *v/v* PBS. Electrospinning was started within 1 minute of addition. Polycaprolactone (PCL; 10% *w/v*) was added to a blend of DCM and DMF (90:10 *v/v*) and stirred at room temperature until dissolved. Hydrophobic backing layers were introduced by subsequent electrospinning of PCL solutions on top of the mucoadhesive layer. The resulting materials were placed in a dry oven at 70 °C for 15 minute to melt the PCL layer into a continuous film [16]. Experimental samples were taken from the central region of the dual-layer patches and the thickness measured 6 times at 1 cm intervals using a digital micrometer (Mitutoyo, Kanagawa, Japan).

2.5. Scanning electron microscopy

Patches were imaged using a TESCAN Vega3 scanning electron microscope (SEM; Tescan, Cambridge, UK). Samples were sputter coated with gold and imaged using an emission voltage of 10 kV. All images were processed using ImageJ software tools [21]. Fibre diameters were measured by ImageJ using randomly generated coordinates and a

superimposed grid to select fibres to measure [22]. Three images were analysed for each composition with at least 10 measurements per image.

2.6. Fabrication and imaging of fluorescent electrospun fibres

Fluorescent electrospun mucoadhesive membranes were prepared as previously described using fluorescein-conjugated goat anti-mouse IgG F(ab) (FITC-F(ab); Abcam, Cambridge, UK). PVP is intrinsically fluorescent, allowing simultaneous imaging of the polymer fibres and FITC-conjugated F(ab) [23]. Samples were placed on glass slides and overlaid with glass cover slips. Imaging was performed in dual-channel mode using a Nikon A1 laser scanning confocal microscope using 403.55 nm and 488 nm sapphire lasers with 450/25 nm and 525/25 nm bandpass filters. All images were processed using ImageJ software tools.

2.7. Release profile of F(ab) from electrospun membranes

Three independently prepared biotinylated-F(ab)-containing or NM patches (as controls) were used to measure F(ab) release profiles in PBS. PCL backing layers were removed from patch samples using forceps and 5 mg samples of mucoadhesive membrane placed in a 12-well plate (pre-blocked with 1% *w/v* BSA overnight at 4 °C) and immersed in 2 mL PBS at 37 °C with shaking. Aliquots of 10 μL were taken at predetermined intervals and stored briefly at 4 °C. Samples were subsequently diluted (1:100) in 1% BSA and antigen-binding concentrations measured by ELISA. Measured antigen binding concentrations were normalised against the hypothetical maximum concentration, determined by the dry mass fraction of F(ab) in the electrospinning solution, to calculate percentage release.

2.8. Qualitative flexibility assessment

A 1 × 12 cm strip intersecting the centre of the electrospun dual-layer sheet was cut by scalpel. Flexibility and handleability testing were performed by firstly folding the strip in half and visually inspecting the mucoadhesive and backing layers for damage or permanent deformation. Secondly, the strip was wrapped around a metal tube (ø 10 mm) and inspected once more. These tests were performed using a dry strip and a wet strip after immersing in PBS for 30 s.

2.9. Patch residence time on ex vivo porcine buccal mucosa

Porcine buccal mucosa was excised from bisected porcine heads immediately after slaughter and buccal mucosal grafts (0.5 mm) taken using a Braithwaite grafting knife (Swann Morton, Sheffield, UK). Samples were sealed in plastic bags, preserved by flash freezing in liquid nitrogen and stored at −80 °C before use. Frozen samples were defrosted in a 37 °C water bath, attached to 100 mm petri dishes using cyanoacrylate glue and the surface of the mucosa moistened using PBS. Circular patch samples (ø 10 mm) were applied using gentle pressure with a gloved fingertip for 5 s. Pre-warmed PBS (30 mL) was added to submerge the samples and the petri dishes shaken on an orbital shaker at 37 °C, 250 rpm. The samples were inspected every 15 minutes for 3 h for detachment of the entire patch or backing layer.

2.10. Cell culture

FNB6-hTERT immortalized oral keratinocytes (FNB6; Ximbio, London, UK) were cultured in a flavin- and adenine-enriched medium consisting of high glucose Dulbecco's modified Eagle's medium (DMEM) and Ham's F12 medium in a 3:1 *v/v* ratio supplemented with 10% *v/v* fetal bovine serum (FBS), epidermal growth factor (10 ng/mL), adenine (0.18 mM), insulin (5 μg/mL), transferrin (5 μg/mL), L-glutamine (2 mM), triiodothyronine (0.2 nM), amphotericin B (0.625 μg/mL), penicillin (100 IU/mL), and streptomycin (100 μg/mL). Normal oral fibroblasts (NOF) were isolated from the connective tissue of biopsies obtained from the oral mucosa of patients during routine dental procedures with written informed consent (Ethical Approval No. 09/H1308/66) and cultured in DMEM supplemented with FBS (10% *v/v*), L-glutamine (2 mM), penicillin (100 IU/mL), and streptomycin (100 μg/mL). Monocyte-derived macrophages (MDM) were differentiated from peripheral blood primary human monocytes as previously described [24]. Briefly, buffy coats obtained from the National Blood Service, UK (Ethical Approval No. 012597) were diluted 1:1 in Hank's balanced salt solution (without Ca^{2+} and Mg^{2+}) and mononuclear cells separated by density-gradient centrifugation using Ficoll® Paque Plus (GE Healthcare, Chalfont Saint Giles, UK). Monocytes were purified by plastic adherence and differentiated to MDM by 7 days culture in Iscove's modified Dulbecco's medium supplemented with human AB serum (2% *v/v*), L-glutamine (2 mM), penicillin (100 IU/mL), and streptomycin (100 μg/mL).

2.11. Generation of oral epithelial equivalents

FNB6 cells (5×10^5 in 0.5 mL) were seeded onto the apical surface of fibronectin-coated (10 μg/mL) 12-well, 0.4 μm pore cell culture inserts (Greiner Bio One Ltd., Stonehouse, UK) and cultured submerged for 2 days, after which the models were raised to an air-liquid-interface and cultured for a further 10 days.

2.12. Transepithelial electrical resistance

Before measurement, FNB6 epithelial models were washed with PBS and placed in a 12-well plate, 0.5 mL PBS was added to basolateral chambers and 0.3 mL to apical chambers. Tissue integrity was assessed by measuring transepithelial electrical resistance (TEER) using an EVOM2 voltmeter (World Precision Instruments, Madison, USA) at three locations per model, and the average of these values calculated. The resistance across the epithelium was obtained by subtracting the resistance value derived from a blank cell culture insert. The following equation was used to calculate TEER: TEER ($\Omega.cm^2$) = Resistance (Ω) × Membrane area (cm^2).

2.13. F(ab) permeation in oral epithelium equivalents

TEER was measured to verify presence of barrier properties and oral epithelial equivalents (OEE) placed in a 12-well plate (pre-blocked with 10% *w/v* BSA overnight at 4 °C) containing 1 mL cell culture medium. Samples containing biotinylated-F(ab) were applied to the apical chamber and the models incubated with shaking. Sample dose forms included F(ab) solutions in PBS (1 μg/mL, 0.5 mL), F(ab) patch (5–7 mg), NM patch (5–7 mg). Patch samples were carefully placed on the apical surface using sterilised forceps without applying additional pressure. PBS (0.1 mL) was added before application of the patches to simulate the moisture of the oral cavity and hydrate the patches. Equivalent patch samples were weighed before and after removal of the backing layer, showing that the adhesive F(ab)-containing layer contributes 62 ± 2% *w/w* to the overall patch. Given a F(ab) content of 130 ng/mg in the adhesive layer, the patches contained doses of 496 ± 49 ng, which is equivalent to those applied as solution (500 ng). Media samples were taken from the basolateral chamber at predetermined intervals and the equivalent volume of media replaced (200 μL). Media samples were stored at −80 °C before measuring F(ab) concentration by ELISA and calculating cumulative amount permeated. Additionally, patches containing FITC-F(ab) were applied identically for 9 h before washing with PBS and fixing in neutral buffered formalin (10% *v/v*) for 24 h. The OEE were sectioned and mounted in antifade mounting medium with DAPI (Vector Laboratories, Upper Heyford, UK) or mounted without sectioning before imaging by laser scanning confocal microscopy.

2.14. Preparation of anti-TNFα F(ab)

Rabbit anti-TNFα IgG (5 mg/mL, 0.25 mL) was fragmented using a Pierce™ F(ab) preparation kit (Thermo Fisher Scientific, Loughborough, UK) as per the manufacturer's instructions. The concentration of the resulting F(ab) was estimated as recommended by the manufacturer from absorbance at 280 nm, assuming an extinction coefficient of 1.4 mL mg^{-1} cm^{-1}. The products were analysed without reduction or denaturation by SDS-PAGE using a NuPAGE™ 4–12% bis-tris gel as directed with NuPAGE™ MOPS running buffer (Thermo Fisher Scientific, Loughborough, UK) and visualised using Expedeon InstantBlue™ Coomassie-based stain (Abcam, Cambridge, UK). The F(ab) product was concentrated using Pierce™ 10 kDa molecular weight cut-off polyethersulfone membrane protein concentrators (Thermo Fisher Scientific, Loughborough, UK) as directed, and the final concentration calculated by mass balance.

2.15. TNFα neutralisation assay

The TNFα neutralising activity of anti-TNFα whole IgG and F(ab) were measured as a decrease in TNFα-mediated CXCL8 release by FNB6 monolayers. FNB6 cells (8×10^4 cells per well) were seeded in 24-well plates and incubated for 18 h until confluent. Samples in PBS were combined 1:1 with cell culture medium with or without recombinant human TNFα (10 ng/mL) and incubated at 37 °C for 1 h to allow any neutralisation to occur. Media were aspirated from the monolayers and the cells treated with either 10 ng/mL recombinant TNFα, F(ab)-neutralised TNFα or medium alone as control for 24 h. CXCL8 in the conditioned media was measured using an ELISA kit (Bio-Techne, Abingdon, UK) as directed. Patch-eluted F(ab) activity was measured in an identical manner. To elute, F(ab) patch and NM patch samples (30 mg) were immersed in 2 mL PBS for 3 h at 37 °C with shaking.

2.16. Effect of electrospun polymers on TNFα concentration

TNFα (1 ng/mL, 1 mL) was added to glass vials with or without samples of NM patch (10 mg). The vials were incubated at 37 °C for 24 h before measuring free TNFα concentration using an ELISA kit (Bio-Techne, Abingdon, UK) as directed.

2.17. Generation and treatment of immunocompetent oral mucosal ulcer equivalents

Immunocompetent oral mucosal ulcer equivalents (OMUE) were constructed as previously described [25]. NOF (2×10^5 cells/mL) and MDM (1×10^6 cells/mL) in cell culture media (1 mL) were added to a collagen gel-forming solution comprising rat tail collagen (3.48 mg/mL), 10 × DMEM (10% *v*/v), FBS (8.3% v/v), L-glutamine (2 mM), sodium bicarbonate (2.3 mg/mL), 4-(2-hydroxyethyl)-1-piperazineethanesulfonic acid (5 mg/mL), sodium hydroxide (0.25 mg/mL). The solution was adjusted to pH 7 by the addition of sodium hydroxide (1 mM) and 1 mL added to 12 mm cell culture inserts. The collagen used in all experiments contained <0.2 EU/mL endotoxin when quantified by limulus amebocyte lysate assay (Thermo Fisher Scientific, Loughborough, UK). The cell-populated collagen hydrogels were incubated in a humidified atmosphere at 37 °C for 2 h to solidify. Sterilised titanium cylinders (ø 5 mm, h 10 mm) were placed on the centre of the hydrogel before seeding FNB6 cells (0.5 mL, 5×10^5) and culturing submerged for 2 days. The models were raised to an air-to-liquid interface and cultured for a further 9 days, after which the titanium cylinders were removed.

OMUE were transferred to a 12-well plate containing cell culture media (1 mL). Models were pre-treated as required for 24 h by applying patch samples carefully to the apical surface using sterilised forceps without applying additional pressure. Lipopolysaccharide (LPS) from *Escherichia coli* 0111:B4 (500 ng/mL; Invitrogen, Waltham, USA) was added as required to the basolateral chambers to simulate an MDM inflammatory response. After 6 h incubation, samples of conditioned media were taken from basolateral chambers and replaced with the equivalent volume of cell media (300 μL). After a further 18 h, the entire conditioned media were collected. Samples were stored at −80 °C until analysis. To test for patch cytotoxicity, full thickness oral mucosal equivalents were treated with either NM or anti-TNFα-loaded patch for 18 h. Receptive medium samples from the lower transwell were tested immediately for lactate dehydrogenase release (CytoTox Non-radioactive Cytotoxicity Assay) as a marker of tissue damage according to the manufacturer's instructions (Promega, Chilworth, UK).

2.18. Cytokine release analysis

TNFα concentrations in conditioned media were measured by ELISA (Bio-Techne, Abingdon, UK) as directed. The C1 human chemokine antibody array (Antibodies-online GmbH, Aachen, Germany) was used to provide semi-quantitative measurements of the concentrations of 38 human chemokines in conditioned media collected after 24 h from immunocompetent OMUE. Membranes were visualised using a C-DiGit blot scanner (Li-cor, Cambridge, UK) and analysed using Quantity One software (Bio-Rad Laboratories, Hercules, USA). Selected chemokines (CCL3, CCL5, CXCL10) were further quantified using ELISA (Bio-Techne, Abingdon, UK). The experiment and ELISA quantification were performed 3 times using different batches of MDM. The presented data are from a single representative batch of MDM.

2.19. Histological analysis

OEE or OMUE were washed with PBS, fixed in neutral buffered formalin (10% *v/v*) for 24 h, and paraffin-wax embedded using standard histology procedures. Sections (5 μm) were cut using a Leica RM2235 microtome (Leica Microsystems, Wetzlar, Germany) and mounted on Superfrost Plus slides (Thermo Fisher Scientific, Loughborough, UK). Sections stained with haematoxylin and eosin were mounted in dibutylphthalate polystyrene xylene and imaged using an Olympus BX51 microscope with cellSens Imaging Software (Olympus GmbH, Hamburg, Germany).

2.20. Data analysis

All data and statistical analyses were performed using GraphPad Prism 9.3 software (GraphPad Software, La Jolla, USA). Unless stated data are presented as mean ± standard deviation of at least three independent experiments. Unpaired Student's *t*-test or one-way ANOVA with Tukey's post-hoc test was used for pairwise or groupwise comparisons and results considered statistically significant if $p < 0.05$. Half-maximal inhibitory concentrations (IC_{50}) were calculated using 4-parameter logistic regression and presented as mean ± SD.

3. Results and discussion

3.1. Stability of biotinylated-F(ab) in ethanol-water mixtures

Electrospinning involves applying a high voltage electric field to an extruded polymer solution, resulting in the production of a micron-scale, non-woven mesh of polymeric fibres [17]. We have utilised electrospinning technology to develop a dual-layer patch for drug delivery to the oral mucosa, which is comprised of a mucoadhesive drug-eluting layer that consists of a blend of poly(vinyl pyrrolidone) (PVP) and Eudragit® RS100 (RS100), and a water-impermeable backing layer made of heat-treated PCL [16]. The high surface area and hydrophilicity of the fibres promotes rapid swelling, efficient drug release while maximising mucoadhesive interactions.

The RS100 polymer is an integral component in the electrospun mucoadhesive layer of the patch, preventing dissolution in saliva and promoting adhesion through electrostatic interactions with mucins.

RS100 is not water soluble and therefore an organic processing solvent such as ethanol is required to dissolve RS100 for electrospinning. Ethanol is generally considered to be a protein denaturant; however, we previously observed that lysozyme could be electrospun into PVP/RS100 fibres from various ethanol-water mixtures without significant loss of enzyme activity [20]. F(ab) antigen binding activity following exposure to different ethanol-water mixtures was measured in order select a solvent composition suitable for F(ab) incorporation. Ethanol concentrations of 40% *v/v* and below did not cause significant F(ab) activity loss. Incubating F(ab) (1 μg/mL) in 97% *v*/v ethanol resulted in a decrease in antigen binding activity to 32 ± 11% of its initial activity ($p < 0.001$). In contrast, use of 80% *v*/v ethanol caused a complete loss of antigen binding ($p < 0.001$), whereas 60% v/v ethanol caused comparable activity loss to 97% *v*/v (Fig. 1). We previously overserved that fibres prepared with <60% v/v ethanol are prone to disintegration in aqueous media [20]. The relatively high F(ab) activity observed at 97% v/v ethanol may be a result of lower solvation of the unfolded protein at high ethanol concentrations, increasing the free energy barrier for ethanol-induced denaturation. Therefore, use of 97% v/v ethanol as the solvent was selected for patch fabrication.

3.2. Encapsulation and release from electrospun patches

Dual layer mucoadhesive electrospun patches were fabricated using a modification to our previously described protocol [20]. Briefly, biotinylated-F(ab) or FITC-F(ab) were incorporated within the adhesive layer by mixing the aqueous F(ab) solution with the ethanolic polymer solution directly before electrospinning, giving a theoretical maximum loading of 130 ng/mg by dry mass in the adhesive layer of the patch. No noticeable difference in fibre morphology between NM patches and biotinylated-F(ab)-loaded patches was observed by SEM (Fig. 2 A-B). Furthermore, the inclusion of F(ab) had little effect on fibre diameter, with NM fibres having an average diameter of 1.82 ± 0.88 μm and biotinylated-F(ab)-containing fibres of 2.31 ± 0.81 μm (Fig. 2C). Dual-layer sheets had a thickness of 307 ± 46 μm and 261 ± 22 μm for the useable area of NM and F(ab)-loaded sheets, respectively.

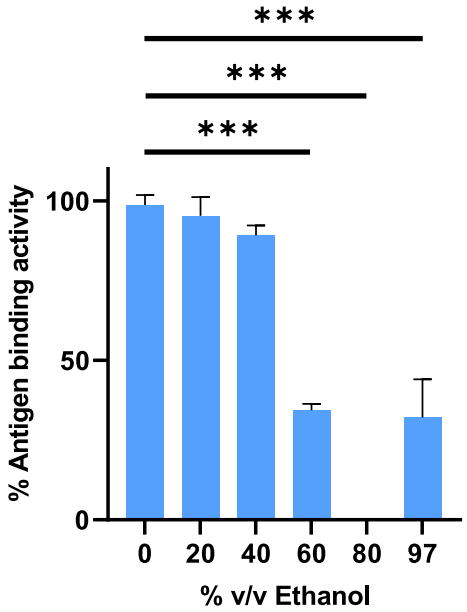

Fig. 1. Antigen binding activity of biotinylated-F(ab) following exposure to increasing ethanol concentrations. F(ab) was added to glass vials containing various ethanol/water mixtures and incubated for 1 h with shaking before measuring antigen binding F(ab) concentration by ELISA. Data are presented as mean ± SD ($n = 3$) and analysed by one-way ANOVA with Dunnett's post-hoc test comparing each group to 0% *v*/v ethanol. ***$p < 0.001$.

FTIC-conjugated F(ab) was also incorporated to visualise the distribution of F(ab) within the fibres by dual-channel confocal microscopy, where patch fibres were imaged making use of the intrinsic fluorescence of PVP (Fig. 2D). Interestingly, micrographs of FITC-conjugated F(ab)-containing fibres revealed that the F(ab) was dispersed throughout the fibres as micro- and nanometre-sized particles/aggregates (Fig. 2E), implying the formation of a colloidal precipitate following addition of the F(ab) to the polymer solution. Dissolved inert polymers, including PVP, are known to induce precipitation of antibodies and large proteins through a volume exclusion effect, whereby proteins are sterically excluded from interacting with the solvent [26,27]. This, along with the reduced solubility of proteins in ethanol, is likely involved in the precipitation mechanism.

Elution of the biotin-conjugated F(ab) from the mucoadhesive layer into PBS revealed complete preservation of antigen binding activity, with 97.1 ± 5.7% of the dose being detectable by ELISA after 3 h (Fig. 2F). This contrasts with the reduced activity observed for F(ab) after incubation in 97% *v/v* ethanol in the absence of polymers. It is likely that PVP stabilises F(ab) by limiting protein-solvent interactions through volume exclusion and by non-specific binding to F(ab) in its native conformation [28]. F(ab) was released rapidly, following first-order kinetics, with 64 ± 16% released within 0.5 h and 89 ± 28% after 1 h. Eluted NM patches produced negligible absorbance across all timepoints. This rapid release is similar to our previous observations for highly soluble proteins [20], and is likely facilitated by rapid swelling of the fibres. Complete release over a short timeframe is appropriate for oromucosal delivery, as patients can only be expected to refrain from eating and drinking for short periods. A mucoadhesive adhesion assay was performed using *ex vivo* porcine buccal mucosa. F(ab)-loaded patches displayed similar mucoadhesive residence times to NM patches (2.75 ± 0.32 h compared to 2.0 ± 1.2 h, respectively; Fig. S2). These residence times are similar to those previously observed in humans [18] and show that inclusion of F(ab) does not adversely affect patch adhesive properties. Flexibility is an important property for oral patches, which must adhere to curved surfaces within the mouth and withstand mechanical forces caused by movement of the tongue and jaw. Qualitative assessment of patch flexibility showed that strips of both F(ab)-loaded and NM patch in either a wet or dry condition could be folded in half or wrapped around a curved surface without breaking or permanently deforming.

Despite strong clinical interest in alternative formulations for antibodies and their derivatives, there have been few studies investigating the encapsulation of antibodies into polymer fibres by electrospinning and none that we are aware of involving F(ab). Gandhi et al. [29], examined the encapsulation of anti-$\alpha_v\beta_3$ integrin IgG within PCL fibres by uniaxial electrospinning from a 60:40 (*w/w*) mixture of dimethylformamide and dichloromethane. Burst release was observed by spectrophotometry followed by a period of sustained release, suggesting initial release driven by desorption from the polymer surface followed by slow release due to fibre degradation. Including bovine serum albumin (BSA) as a porogen facilitated anti-$\alpha_v\beta_3$ release, with 51% release being observed after 4 h at the highest BSA loading. Although the solvents used are generally considered to be denaturing, at least some antigen binding activity was maintained, as shown by the antigen-specific staining of integrin-expressing endothelial cell monolayers [29]. Notably, Angkawinitwong et al., encapsulated bevacizumab, a monoclonal antibody (mAb) that binds to and inhibits vascular endothelial growth factor A thereby reducing angiogenesis, within PCL core-shell fibres by coaxial electrospinning. The use of an aqueous core-forming solution enabled preservation of antigen binding activity, as confirmed by surface plasmon resonance. As is typical of coaxial fibres, slow zero-order release was observed over a 2-month period, suggesting a potential application as an implantable material for sustained antibody release [30].

Shelf-life is another important consideration in developing solid dosage forms for biologic delivery. In general, immobilisation of

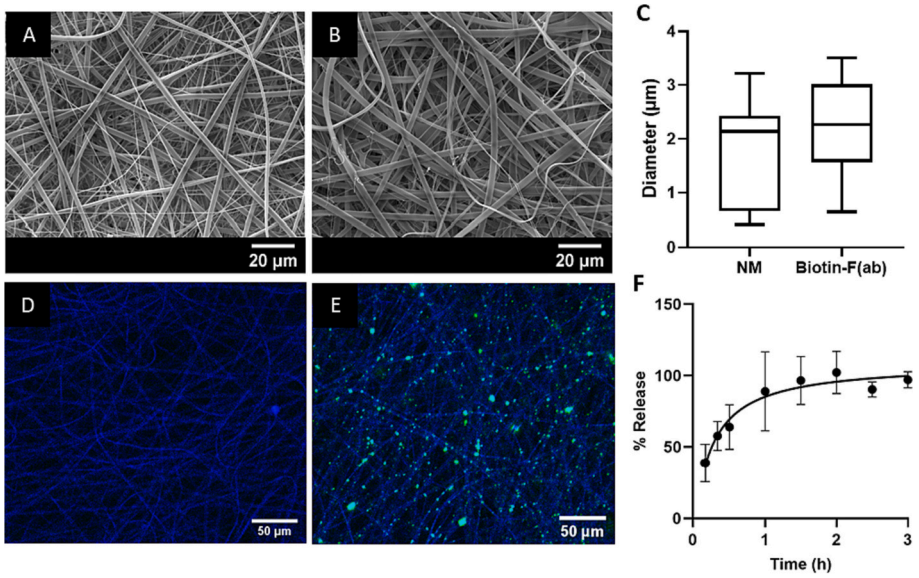

Fig. 2. Incorporation by electrospinning and release of F(ab) from mucoadhesive patches. Scanning electron micrographs of mucoadhesive electrospun (A) NM and (B) biotin-conjugated F(ab)-containing fibres. (C) Fibre diameter distributions presented as median, interquartile range, and range ($n = 30$). (E) Confocal micrographs of mucoadhesive electrospun (D) NM and (E) FITC-conjugated F(ab)-containing fibres. (F) Release of biotinylated F(ab) from mucoadhesive membranes following immersion in PBS. Presented as mean ± SD (n = 3).

proteins within a solid formulation can often improve shelf-life by preventing aggregation [31]. Indeed, lyophilisation in the presence of cryoprotectants can considerably increase the shelf-life of many antibodies [32]. Despite this, existing therapeutic antibodies are exclusively delivered as liquids [33] and there have been few detailed studies on the stability of antibodies within polymer-based solid formulations. Frizzell et al., observed that the shelf-lives of horseradish peroxidase and alkaline phosphatase are improved by encapsulating within electrospun

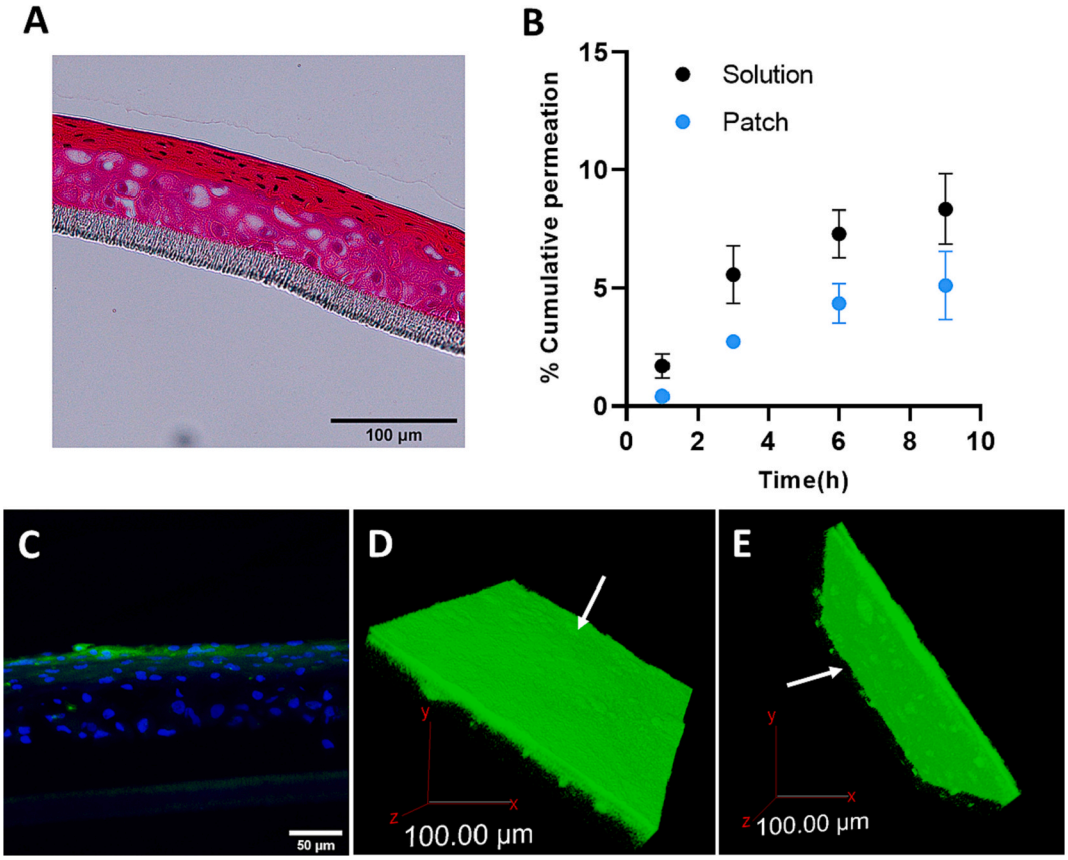

Fig. 3. F(ab) permeates the oral epithelium when applied as either a patch or solution. Patches and solutions containing biotinylated F(ab) were applied to the apical side of oral epithelial equivalents (OEE). (A) Representative haematoxylin and eosin stain of an OEE. Transepithelial permeation was measured by periodically measuring F(ab) concentration in the basolateral chamber. (B) Plot of cumulative percentage transepithelial biotinylated F(ab) permeation when applied to OEE as solution or patch. Data are presented as mean ± SD ($n = 3$). Patches containing FITC-F(ab) were applied to OEE for 9 h, formalin fixed, and the distribution of FITC-F(ab) visualised by confocal microscopy. (C) Cross section showing distribution of FITC-F(ab) (green) with DAPI nuclear counterstain (blue). Three-dimensional projections showing the distribution of FITC-F(ab) with white arrows indicating the (D) apical and (E) basolateral surface of the OEE.

polymer fibres and can be further extended by lyophilisation to remove residual water from the material [34]. Packaging with dry nitrogen and cold storage are routinely used in the pharmaceutical industry and might be considered to improve the shelf-life if required. Detailed studies on stability and storage conditions of antibody-based therapeutics within solid formulations would be beneficial and necessary for clinical translation.

The release rate and high antigen binding activity indicate that our formulation is promising for mucosal F(ab) delivery. The high preservation of protein function suggests that uniaxial electrospinning using organic solvents could be considered for the encapsulation of other complex biomacromolecules, as the denaturing effect of solvents that would otherwise be incompatible may be counteracted in the presence of stabilising polymers.

3.3. Delivery of F(ab) to oral epithelium equivalents

The intact oral epithelium is generally considered to be an efficient barrier against the permeation of hydrophilic molecules [35]. However, some small proteins, such as glucagon-like-peptide 1 and insulin, can permeate sufficiently to achieve therapeutically relevant blood serum concentrations [36,37]. The basal epithelium and lamina propria are the primary target for topical delivery to treat most oromucosal diseases. In severe RAS and OLP the epithelium is absent or eroded at the affected site, resulting in impaired barrier function. For successful delivery, an anti-TNFα agent would have to permeate the loose connective tissue of the lamina propria in order to neutralise cytokines in the inflammatory infiltrate. Ideally, it would also permeate the epithelium at least somewhat, to allow the continued treatment of partially regenerated epithelia during wound healing. To assess the ability of the patches to deliver F(ab) to a mucosal surface, tissue engineered OEE were used as a model barrier. The OEE consist of a stratified squamous layer of oral keratinocytes 60–80 μm in thickness (Fig. 3A). Although thinner than native healthy buccal mucosa, the OEE covered the entire insert and had an average TEER of 444 ± 74 Ω cm^2. This value is comparable to or higher than those typically observed for similar 3D oral epithelial models and suggests suitable barrier properties [38].

Patch samples and solutions containing an equivalent dose of biotinylated F(ab) were applied to OEE and the concentration of F(ab) in the basolateral chamber monitored over time (Fig. 3B). At earlier timepoints, permeation of F(ab) applied by patch was delayed compared to F(ab) applied by solution. This is likely caused by the additional time taken for F(ab) to be released from the patch fibres. After 9 h, similar levels of cumulative permeation were achieved corresponding to 5.1 ± 1.5% and 8.4 ± 1.5% of the total dose for F(ab) applied in a patch or solution, respectively. Patches containing FITC-F(ab) were applied to OEE for 9 h before fixing in formalin to immobilise any F(ab) present within the tissue. Confocal microscopy (Fig. 3C) followed by z-stack analysis (Fig. 3D-E) performed on sections, showed that F(ab) mainly accumulated within the upper 3–6 cell layers of the superficial epithelium but could also be detected in isolated regions throughout the lower layers of the OEE.

The data presented here provide the first evidence that biologics can be delivered efficiently to oral epithelia using mucoadhesive patches, with the patches performing comparably to an equivalent solution. In practise, oral rinses would be unsuitable for the delivery of biologics to the oral mucosa due to short exposure times and lack of site-specificity. Whereas, similar dual-layer patches with hydrophobic backing layers have recently been shown to be highly effective for promoting the retention of biologics on the oral mucosa in the presence of saliva flow [39]. To our knowledge, there are no previous studies investigating antibody delivery to the oral mucosa. Saltzman and *co*-workers observed that radiolabelled IgG applied *in vivo* to mouse vaginal mucosa using polymer discs permeated to a similar extent, reaching peak serum concentrations corresponding to approximately 1% of the total dose [40,41]. The higher permeating dose observed in this study may be due to the smaller size of F(ab), leading to increased permeability through the intracellular space, or the absence of additional biodistribution and elimination effects that would be present *in vivo*. Although the F(ab) permeated the top layers of the oral mucosal epithelium in our study, its presence in the lower layers and the levels of complete transepithelial delivery across intact epithelium were somewhat low, as might be expected due to the high permeability barrier this tissue has to high molecular weight proteins. However, as mentioned previously, in most oral mucosal inflammatory lesions the mucosal barrier is absent suggesting that topical F(ab) treatment may be feasible for these types of erosions and ulcers.

3.4. Preparation and activity of neutralising anti-TNFα F(ab)

TNFα neutralising agents are currently one of the most common classes of monoclonal antibody therapy [42]. They are available as whole IgG and other derivatives. Due to their smaller size, F(ab)s, such as certolizumab pegol, are expected to penetrate tissue more easily and therefore should be better suited for topical delivery [43]. A polyclonal neutralising rabbit anti-TNFα IgG was fragmented by enzymatic degradation with papain to generate a F(ab) to serve as a model biological therapeutic for this study. Fc and any unreacted whole IgG were separated from F(ab) by binding to immobilised protein A. Non-denaturing SDS-PAGE indicated the complete separation of the F(ab) and Fc fragments (Fig. 4A). The neutralising activities of the anti-TNFα F(ab) compared to whole IgG were measured by pre-incubating each with 5 ng/mL recombinant TNFα before adding to FNB6 oral keratinocyte monolayers, which are known to secrete CXCL8 in response to TNFα stimulation [44]. The neutralising activity of each antibody species was confirmed as a dose-dependent decrease in TNFα-mediated CXCL8 secretion, as detected by ELISA (Fig. 4B–C). Whole IgG exhibited an IC_{50} concentration of 1.08 ± 0.46 μg/mL, corresponding to a molar IgG to TNFα ratio of 74 ± 30 (assuming IgG and TNFα molecular weights of 150 kDa and 51 kDa respectively). F(ab) had an IC_{50} concentration of 1.45 ± 0.50 μg/mL, corresponding to a molar F(ab) to TNFα ratio of 295 ± 102 (assuming F(ab) molecular weight of 50 kDa). The higher stoichiometric ratio required for neutralisation with the F(ab) may be due to its univalency in comparison to the bivalency of whole IgG. It cannot be presumed that fragmentation of a neutralising antibody will yield a F(ab) with equivalent neutralising activity, as some neutralisation mechanisms rely on bivalency for crosslinking or increased avidity [45]. In this case, the resulting F(ab) maintained TNFα neutralising activity, suggesting utility as a model F(ab) biologic. The relatively high molar excess required for neutralisation is typical of affinity purified polyclonal antibodies, since not all binding will occur *via* epitopes that block activity. It is likely that approved monoclonal F(ab) drugs would have higher potencies because of their single-epitope specificity and optimised binding affinity, however, their availability to researchers is often limited.

3.5. Patch TNFα neutralising activity

Anti-TNFα F(ab) was electrospun into mucoadhesive patches at a theoretical maximum loading of 920 ng/mg by dry mass in the adhesive layer. Activity of the F(ab) following 3 h elution in PBS was measured by neutralisation of TNFα-mediated CXCL8 release by FNB6 monolayers (Fig. 5). Stimulating FNB6 oral keratinocytes with TNFα resulted in a significant increase in CXCL8 secretion from 0.093 ± 0.043 ng/mL to 1.68 ± 0.42 ng/mL ($p < 0.001$). Pre-incubation of TNFα with NM patch eluate reduced CXCL8 levels to 1.24 ± 0.31 ng/mL, although this was not statistically significant ($p = 0.22$). In contrast, preincubation with 10 μg/mL of an anti-TNFα F(ab) solution reduced CXCL8 secretion to baseline levels (0.078 ± 0.044 ng/mL, $p < 0.001$ relative to NM). Similarly, patch-eluted F(ab), with a theoretical maximum concentration of 8.3 μg/mL, also reduced CXCL8 secretion to baseline levels (0.115 ± 0.022 ng/mL, $p < 0.001$ relative to NM). Solutions containing

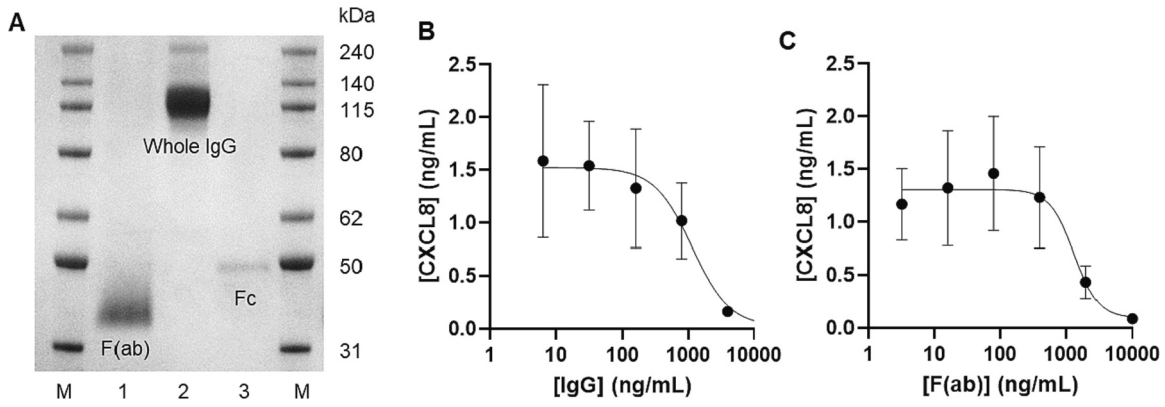

Fig. 4. Preparation and cytokine neutralising activity of anti-TNFα F(ab) as shown by the suppression of TNFα-mediated CXCL8 release. (A) Representative non-reducing SDS-PAGE analysis of papain-fragmented neutralising anti-TNFα IgG. (Lane 1) Purified F(ab) product, (Lane 2) whole IgG starting material, (Lane 3) Fc product, (M) molecular weight marker in kDa. Dose-response curve showing neutralisation of TNFα by (B) anti-TNFα whole IgG and (C) anti-TNFα F(ab) as a decrease in TNFα-mediated CXCL8 release by FNB6 keratinocyte monolayers. Data are presented as mean ± SD ($n = 3$).

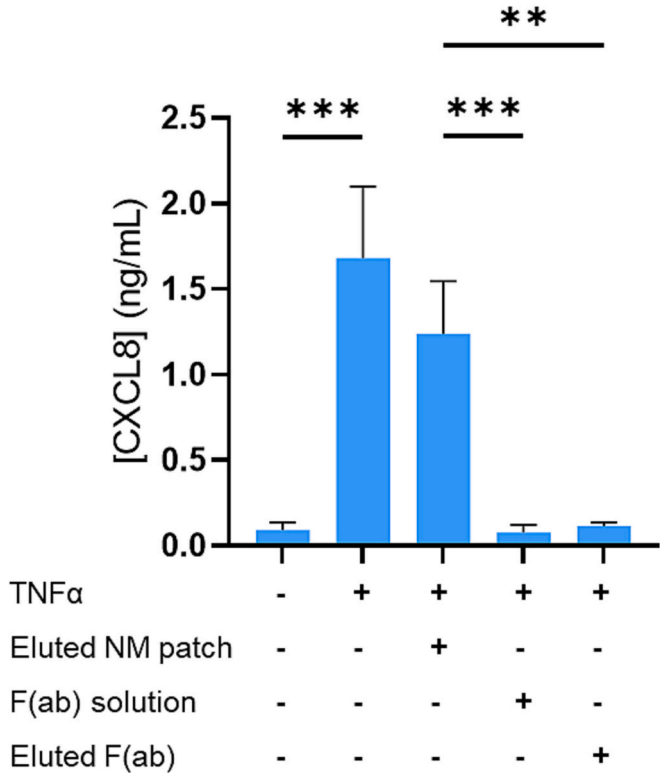

Fig. 5. Patch eluted F(ab) neutralises the activity of TNFα. Patch samples were eluted in PBS and the resulting eluates and controls were preincubated with TNFα before adding to FNB6 monolayers. TNFα neutralisation was detected as a decrease in TNFα-mediated CXCL8 release as measured by ELISA. Data are presented as mean ± SD ($n = 3$) and analysed by one-way ANOVA with Tukey's *post hoc* tests. **, $p < 0.01$; ***, $p < 0.001$.

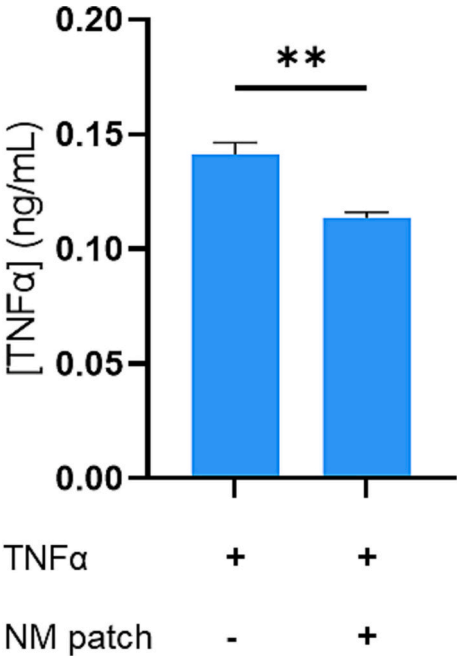

Fig. 6. Free TNFα concentration is reduced by contact with the patch. TNFα solutions were incubated 24 h in glass vials with or without samples of NM patch before measuring TNFα concentrations by ELISA. Data are presented as mean ± SD (n = 3) and analysed by unpaired *t*-test. **, $p < 0.01$.

TNFα (1 ng/mL) were also incubated with and without samples of NM patch at 37 °C for 24 h before measuring TNFα concentration in the media by ELISA (Fig. 6). Interestingly, the presence of the NM patch caused a small but significant decrease in TNFα concentration from 0.1413 ± 0.0051 ng/mL to 0.1135 ± 0.0026 ng/mL ($p < 0.01$), suggesting that the polymers in the patch itself affect active cytokine concentrations, likely through non-specific binding to proteins, which may explain the reduced levels of CXCL8 by FNB6 monolayers incubated with MN elute alone.

These results show that the mucoadhesive patch is suitable for releasing F(ab) with cytokine neutralising activity. CXCL8 is a neutrophil chemokine and although its secretion in 2D keratinocyte monolayers is highly sensitive to TNFα, its concentration is not typically elevated in OLP lesions, suggesting that it is unlikely to be a major driver of oral mucosal ulceration [46]. Furthermore, we have previously observed that CXCL8 secretion is significantly higher and affected to a lesser degree by immune challenge in 3D cultures in comparison to 2D cultures [25]. This emphasizes the importance of further investigation in a 3D disease-relevant model.

3.6. Oral mucosal ulcer equivalents

TNFα and several other chemokines are upregulated in the diseased tissue of patients suffering from oral mucosal inflammatory diseases, where they promote the recruitment and proliferation of cytotoxic T-cells, thus leading to the destruction of the basal epithelium and ulcer

formation [4,46]. We hypothesized that application of a topical anti-TNFα agent could have a potentially therapeutic effect by neutralising macrophage-released TNFα, causing a decrease in detectable TNFα concentrations and reverting secretion of TNFα-sensitive T-cell chemokines to baseline levels. The lack of clinically relevant oral disease models for the investigation of anti-inflammatory drugs is a major barrier to the investigation of anti-inflammatory drugs. There are currently no suitable *in vivo* animal models of OLP and RAS. In addition, small animal models may be inappropriate for studying targeted immunotherapies due to differences in innate immunity between rodents and humans [47]. Tissue-engineered oral mucosal equivalents, typically consisting of a fibroblast-populated collagen hydrogel seeded with keratinocytes and differentiated into a stratified squamous epithelium, are therefore increasingly being used to study disease processes in the oral mucosa [48–52]. To test for biocompatibility, levels of lactate dehydrogenase (as a measure of tissue damage) were measured in the transwell receptive medium following incubation of tissue engineered oral mucosal equivalents with topically applied NM and anti-TNFα F(ab)-containing patches and compared to control untreated models. We found no statistically significant difference between lactate dehydrogenase levels in any of the samples tested (OD_{492nm} untreated control 1.33 ± 0.13, non-medicated patch 1.48 ± 0.08 and F(ab) patch 1.66 ± 0.19), These data are similar to those previously published for similar patches containing clobetasol propionate [18], indicating that these patches are biocompatible.

We recently developed and characterised an immunocompetent oral mucosal equivalent containing primary monocyte-derived macrophages (MDM) [25]. These MDM specifically secreted TNFα in response to bacterial LPS, which then increased the gene expression and secretion of downstream chemokines, molecules known for the chemoattractant properties that are instrumental in driving leukocyte migration to inflammatory sites. Given the central role of TNFα-secreting immune cells, including macrophages [53], in the progression of RAS and OLP, this model is uniquely applicable for investigating novel therapies for these chronic inflammatory diseases.

RAS and ulcerative OLP produce areas of oral mucosa that are denuded of oral epithelium. In the case of RAS, the deleterious actions of both TNFα and cytotoxic T-cells result in round shallow ulcers, often covered by a thin layer of fibrin (Fig. 7Ai). Histologically, these lesions show exposed connective tissue populated by cytokine secreting leukocytes that perpetuate the disease, with epithelium only present at the edge of the ulcer (Fig. 7Aii). To replicate these lesions *in vitro* we cultured immunocompetent oral mucosal models in the presence of a 5 mm diameter titanium cylinder to occlude epithelial growth in a defined area (Fig. 7B). Removal of cylinders produced OMUE that resemble aphthous or OLP ulcers, with exposed simulated connective tissue, consisting of a fibroblast- and macrophage-populated collagen hydrogel. Above and at the edge of the ulcer is a stratified epithelium of oral keratinocytes (Fig. 7C) analogous to human ulcers. Aphthous ulcers typically have diameters ranging from 8 mm to 1 cm; severe OLP produces irregularly shaped ulcers with an area of approximately 60 mm^2 [19,54]. Therefore, the resulting area of exposed connective tissue in the OMUE is a conservative representation of that which would be present in patients and provides a useful model with impaired barrier function for investigating treatments for ulcerative oral mucosal diseases.

3.7. *Effect of patch application on cytokine release from immunocompetent oral mucosal ulcer equivalents*

To investigate their effect in a disease model, TNFα-neutralising

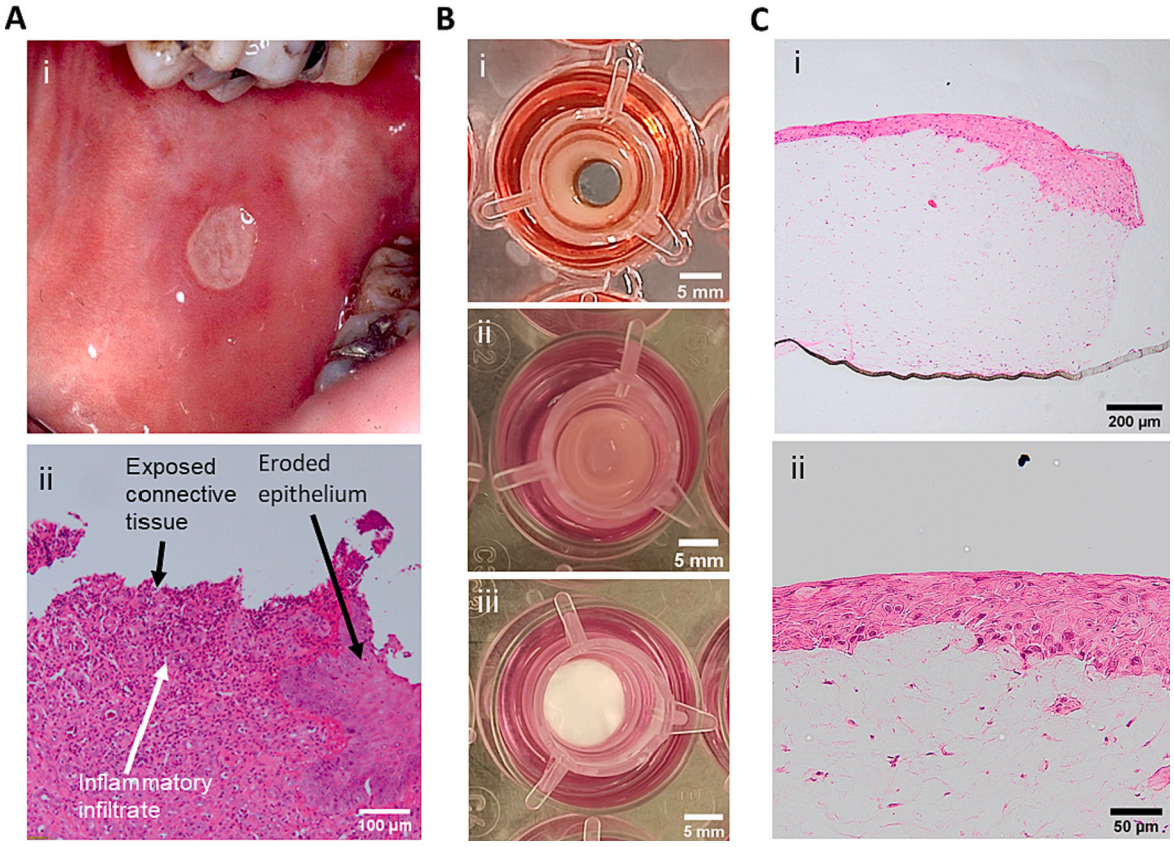

Fig. 7. Histological and photographic comparison of oral aphthous ulcers and tissue engineered immunocompetent ulcer equivalents. (Ai) Photograph of oral aphthous ulcer. (Aii) Haematoxylin and eosin stain of oral aphthous ulcer biopsy. Photographs of tissue engineered oral mucosal ulcer equivalents (Bi) before and (Bii) after removal of titanium cylinder and (Biii) after application of anti-TNFα F(ab) patch. (Ci, Cii) Haematoxylin and eosin stains of oral mucosal ulcer equivalent. (Image in Ai courtesy of Prof. Martin Thornhill, University of Sheffield, image in Aii courtesy of Dr. Ali Khurram University of Sheffield).

patches and NM patches were applied to OMUE for 24 h after which LPS was added to the media in the basolateral chamber to induce an immune response. MDM in 3D oral mucosal equivalents are known to secrete TNFα in response to LPS [25]. After 6 h, LPS stimulation in untreated OMUE caused a large increase in TNFα concentration to 1.67 ± 0.63 ng/mL compared to 0.116 ± 0.017 ng/mL for unstimulated OMUE (Fig. 8A; $p < 0.01$). Pre-treatment with TNFα-neutralising patches reduced TNFα concentrations to baseline levels of 0.30 ± 0.16 ng/mL ($p < 0.05$). Here, the anti-TNFα adheres to the TNFα released by MDM, preventing its binding to capture/detection antibodies in the ELISA, resulting in apparent decreased TNFα levels. TNFα concentrations at 24 h were mostly comparable to those at 6 h (Fig. 8B). OMUE treated with NM patches produced variable TNFα concentrations of 0.77 ± 0.45 ng/mL and 0.94 ± 0.56 ng/mL after 6 h and 24 h respectively. These data suggest successful delivery of potentially therapeutic doses anti-TNFα F(ab), sufficient to bind the secreted TNFα almost entirely.

The concentrations of chemokines in the media 24 h after LPS stimulation were profiled using a protein array (Fig. 9A-B). T-cell chemokines CCL3, CCL5 and CXCL10 were identified as having markedly increased levels in response to LPS stimulation and therefore these chemokines were further quantified by ELISA (Fig. 9 Ci-ii). CCL5 and CXCL10 have also been strongly implicated in the pathogenesis of OLP (Fig. 9Ciii) [55]. CCL3 concentrations were increased from 0.30 ± 0.11 to 5.9 ± 1.4 ng/mL in response to LPS stimulation ($p < 0.01$). Interestingly, treatment with either NM or anti-TNFα patches reduced CCL3 levels to approximately 2 ng/mL ($p < 0.05$). CCL3 belongs to the family of macrophage inflammatory proteins which promote cytotoxic T-cell recruitment and are secreted by several cell types including macrophages, monocytes, and fibroblasts [56]. Monocytes and macrophages express CCL3 in response to LPS stimulation [57], through a process at least partially mediated by TNFα [58]. Similarly, CCL5 concentrations were increased from 1.04 ± 0.22 to 2.28 ± 0.15 ng/mL by LPS stimulation ($p < 0.01$). Treatment with either NM patch or anti-TNFα patch reduced CCL5 to baseline concentrations ($p < 0.01$, $p < 0.001$). CCL5 is a potent T-cell chemokine abundantly expressed by oral keratinocytes in response to TNFα [59], as well as by fibroblasts, T-cells, and macrophages [60]. It has elevated levels in the oral epithelium and lamina propria of OLP biopsies [4]. CXCL10 concentrations were increased from 1.871 ± 0.098 to 2.30 ± 0.19 ng/mL by LPS stimulation ($p < 0.05$). Treatment with anti-TNFα patch reduced CXCL10 to baseline levels of 1.769 ± 0.059 ng/mL ($p < 0.05$).

These data show successful reduction in TNFα, CCL3, CCL5, and CXCL10 close to baseline levels in response to anti-TNFα patch treatment. Interestingly, NM patches also had some effect on cytokine and chemokine concentrations, with CCL3 and CCL5 both being significantly reduced by NM patch treatment, although levels in NM patch-treated OMUEs were variable. The patches likely reduce pro-inflammatory cytokine levels through a combination of selective neutralisation of TNFα by the released biologic and an anti-inflammatory effect caused by non-specific cytokine binding by the patch polymers. Interestingly, during a phase II clinical trial involving the same patches but containing clobetasol for delivery to OLP ulcers, both clinicians and patients reported that the non-medicated (NM) patches used as a placebo were beneficial for the management of OLP [19]. The PVP polymer used in these patches is also routinely used in cutaneous wound dressings and PVP-containing films were recently found to reduce inflammatory cytokine levels, including TNFα, and promote wound healing in a diabetic mouse model [61]. Similarly, PVP-coated nanoparticles have also been observed to reduce TNFα levels when added to bacteria-infected macrophages [62]. To our knowledge there are no other studies that have investigated topical delivery of cytokine neutralising antibodies for the treatment of oral mucosa diseases. Burgess et al. conducted a phase I clinical trial on an inhalable powder containing neutralising anti-IL-13 F(ab) for the treatment of asthma. The treatment was well tolerated and reduced exhaled nitric oxide levels, providing evidence of anti-inflammatory effect in the respiratory epithelium [63]. The suppression of these key disease-causing cytokines represents the first experimental evidence in support of topical anti-TNFα therapy to treat ulcerative oral diseases.

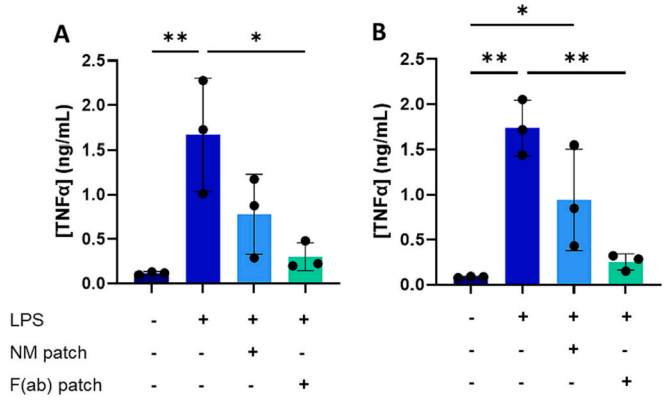

Fig. 8. Patches applied to immunocompetent oral ulcer models neutralise LPS-mediated TNFα release. NM and anti-TNFα F(ab)-containing patches were applied to OMUE for 24 h before stimulating with LPS. TNFα concentrations (A) 6 h and (B) 24 h following LPS stimulation. Data are presented as mean ± SD ($n = 3$) and analysed by one-way ANOVA with Tukey's *post hoc* tests. *, $p < 0.05$; **, $p < 0.01$.

4. Conclusions

F(ab) were successfully electrospun into mucoadhesive fibres using 97% *v*/v ethanol as a processing solvent. The antibody fragments were retained within the fibres as aggregates and were eluted at a clinically suitable rate with negligible activity loss. F(ab)-containing and non-medicated patches were tested using an *in vitro* oral epithelium model, resulting in transepithelial permeation and detectable levels of F(ab) present within the tissue. Patches containing anti-TNFα F(ab) neutralised the activity of TNFα, as shown by the suppression of TNFα-mediated CXCL8 release from oral keratinocytes grown as monolayer cultures. Patches applied to immune-stimulated oral mucosal ulcer models reduced detectable levels of inflammatory cytokines TNFα, CCL3, CCL5, and CXCL10 to baseline levels. These molecules are major drivers in the pathogenesis of oral ulceration; therefore, this study provides the first experimental evidence to support the efficacy of topical anti-TNFα therapy. This novel approach could improve interventions for debilitating oral diseases such as OLP and RAS, as well as representing a platform technology for the site-specific delivery of antibody fragments to tissue surfaces to treat a wide range of conditions.

CRediT authorship contribution statement

Jake G. Edmans: Conceptualization, Methodology, Investigation, Writing – original draft. **Bethany Ollington:** Methodology, Investigation, Writing – review & editing. **Helen E. Colley:** Conceptualization, Methodology, Supervision, Project administration, Writing – review & editing, Funding acquisition. **Martin E. Santocildes-Romero:** Supervision, Writing – review & editing. **Lars Siim Madsen:** Supervision, Writing – review & editing. **Paul V. Hatton:** Conceptualization, Methodology, Supervision, Writing – review & editing, Funding acquisition. **Sebastian G. Spain:** Conceptualization, Supervision, Writing – review & editing. **Craig Murdoch:** Supervision, Methodology, Writing – original draft, Writing – review & editing.

Declaration of Competing Interest

The authors declare the following financial interests/personal relationships which may be considered as potential competing interests: The research presented was funded, in part, by AFYX Therapeutics APS.

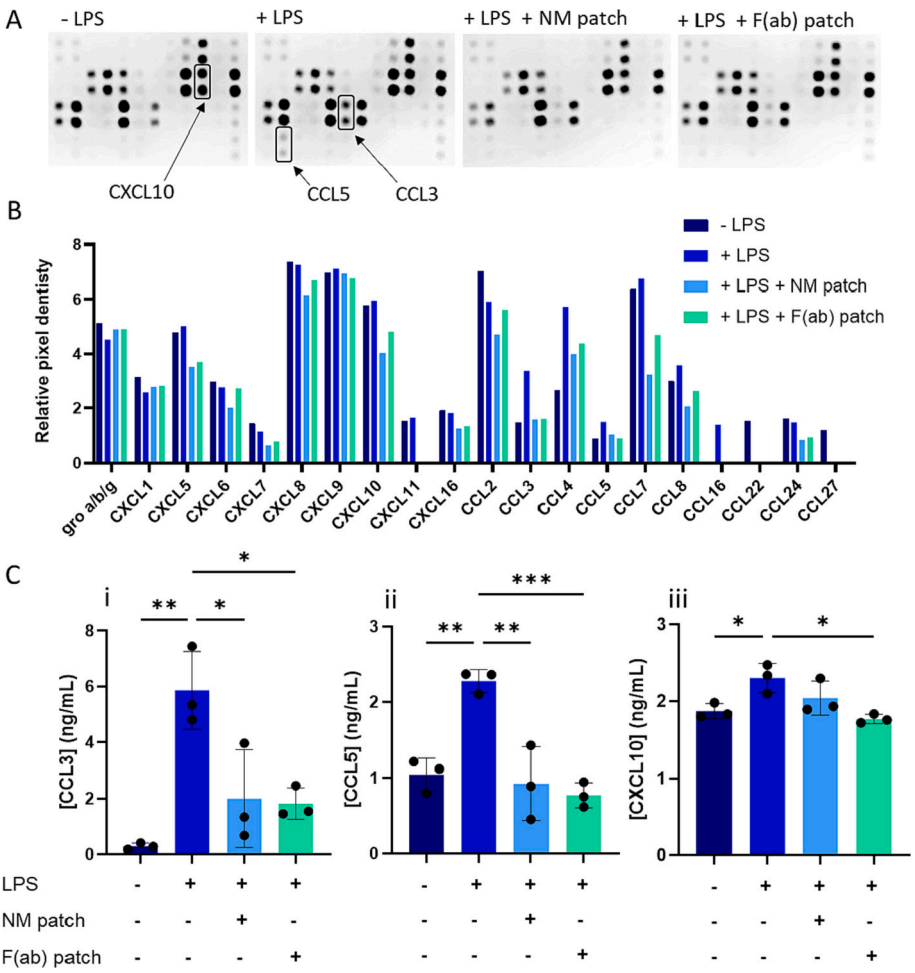

Fig. 9. Effect of patch treatment on chemokine release. NM patches and anti-TNFα F(ab)-containing patches were applied to OMUE for 24 h before stimulating with LPS. After 24 h, chemokine release into the media was profiled using a protein array and selected chemokines quantified by ELISA. (A) Scanned images of protein array membranes. (B) Semi-quantitative densitometric analysis of the array membranes, showing relative chemokine concentrations ($n = 1$). Concentrations of (Ci) CCL3, (Cii) CCL5, and (Ciii) CXCL10 were measured by ELISA. ELISA data are presented as mean ± SD ($n = 3$) and analysed by one-way ANOVA with Tukey's *post hoc* tests. *, $p < 0.05$; **, $p < 0.01$; ***, $p < 0.001$.

JE, BO, HEC, SS and CM declare that they have no other known competing financial interests or personal relationships that could have appeared to influence the work reported within this paper. MES and LSM are employed by AFYX Therapeutics. PVH is on the AFYX Therapeutics APS scientific advisory board, where AFYX have translated mucoadhesive electrospun patch technology for clinical use and have intellectual property (international patent applications WO 2017/085262 A, WO 2021/072113 A1).

Acknowledgements

The authors would like to thank Prof. Keith Hunter (University of Sheffield) for use of the FNB6 oral keratinocyte cell line. Confocal microscopy was performed at the Wolfson Light Microscope Facility where the microscope was purchased with funding from the Wellcome Trust [WT093134AIA, London, UK]. This work was funded by the Engineering and Physical Sciences Research Council [EP/L016281/1, London, UK] as a CASE PhD studentship with the Centre for Doctoral Training in Polymers, Soft Matter & Colloids where AFYX Therapeutics (Copenhagen, Denmark), was the industrial partner.

Appendix A. Supplementary data

Supplementary data to this article can be found online at https://doi.org/10.1016/j.jconrel.2022.08.016.

References

[1] C. Scully, S. Porter, Oral mucosal disease: recurrent aphthous stomatitis, Br. J. Oral Maxillofac. Surg. 46 (2008) 198–206.
[2] M.Á. González-Moles, S. Warnakulasuriya, I. González-Ruiz, L. González-Ruiz, Á. Ayén, D. Lenouvel, I. Ruiz-Ávila, P. Ramos-García, Worldwide prevalence of oral lichen planus: a systematic review and meta-analysis, Oral Dis. 27 (2021) 813–828.
[3] L.J. Taylor, J. Bagg, D.M. Walker, T.J. Peters, Increased production of tumour necrosis factor by peripheral blood leukocytes in patients with recurrent oral aphthous ulceration, J. Oral Pathol. Med. 21 (1992) 21–25.
[4] A. El-Howati, M.H. Thornhill, H.E. Colley, C. Murdoch, Immune mechanisms in oral lichen planus, Oral Dis. 0–3 (2022).
[5] C. Scully, M. Carrozzo, Oral mucosal disease: lichen planus, Br. J. Oral Maxillofac. Surg. 46 (2008) 15–21.
[6] D. Farhi, N. Dupin, Pathophysiology, etiologic factors, and clinical management of oral lichen planus, part I: facts and controversies, Clin. Dermatol. 28 (2010) 100–108.
[7] R. Fischer, R.E. Kontermann, K. Pfizenmaier, Selective targeting of TNF receptors as a novel therapeutic approach, Front. Cell Dev. Biol. 8 (2020) 1–21.
[8] E. Georgakopoulou, C. Scully, Biological agents: what they are, how they affect oral health and how they can modulate oral healthcare, Br. Dent. J. 218 (2015) 671–677.
[9] S. Gupta, S. Ghosh, S. Gupta, Interventions for the management of oral lichen planus: a review of the conventional and novel therapies, Oral Dis. 23 (2017) 1029–1042.
[10] V. Sankar, V. Hearnden, K. Hull, D.V. Juras, M. Greenberg, A. Kerr, P. Lockhart, L. Patton, S. Porter, M. Thornhill, Local drug delivery for oral mucosal diseases: challenges and opportunities, Oral Dis. 17 (2011) 73–84.
[11] I.D. O'Neill, C. Scully, Biologics in oral medicine: ulcerative disorders, Oral Dis. 19 (2013) 37–45.
[12] M. Streit, Z. Beleznay, L.R. Braathen, Topical application of the tumour necrosis factor-α antibody infliximab improves healing of chronic wounds, Int. Wound J. 3 (2006) 171–179.
[13] J. Autio-Gold, The role of chlorhexidine in caries prevention, Oper. Dent. 33 (2008) 710–716.

[14] M. Innocenti, G. Moscatelli, S. Lopez, Efficacy of gelclair in reducing pain in palliative care patients with oral lesions, J. Pain Symptom Manag. 24 (2002) 456–457.

[15] R.J. Bensadoun, J. Daoud, B. El Gueddari, L. Bastit, R. Gourmet, A. Rosikon, C. Allavena, P. Céruse, G. Calais, P. Attali, Comparison of the efficacy and safety of miconazole 50-mg mucoadhesive buccal tablets with miconazole 500-mg gel in the treatment of oropharyngeal candidiasis: a prospective, randomized, single-blind, multicenter, comparative, phase III trial in patients, Cancer 112 (2008) 204–211.

[16] M.E. Santocildes-Romero, L. Hadley, K.H. Clitherow, J. Hansen, C. Murdoch, H. E. Colley, M.H. Thornhill, P.V. Hatton, Fabrication of electrospun mucoadhesive membranes for therapeutic applications in oral medicine, ACS Appl. Mater. Interfaces 9 (2017) 11557–11567.

[17] J.G. Edmans, K.H. Clitherow, C. Murdoch, P.V. Hatton, S.G. Spain, H.E. Colley, Mucoadhesive electrospun fibre-based technologies for oral medicine, Pharmaceutics 12 (2020) 1–21.

[18] H.E. Colley, Z. Said, M.E. Santocildes-Romero, S.R. Baker, K. D'Apice, J. Hansen, L. S. Madsen, M.H. Thornhill, P.V. Hatton, C. Murdoch, Pre-clinical evaluation of novel mucoadhesive bilayer patches for local delivery of clobetasol-17-propionate to the oral mucosa, Biomaterials 178 (2018) 134–146.

[19] M.T. Brennan, L.S. Madsen, D.P. Saunders, J.J. Napenas, C. McCreary, R. Ni Riordain, A.M.L. Pedersen, S. Fedele, R.J. Cook, R. Abdelsayed, M.T. Llopiz, V. Sankar, K. Ryan, D.A. Culton, Y. Akhlef, F. Castillo, I. Fernandez, S. Jurge, A. R. Kerr, C. McDuffie, T. McGaw, A. Mighell, T.P. Sollecito, T. Schlieve, M. Carrozzo, A. Papas, T. Bengtsson, I. Al-Hashimi, L. Burke, N.W. Burkhart, S. Culshaw, B. Desai, J. Hansen, P. Jensen, T. Menné, P.B. Patel, M. Thornhill, N. Treister, T. Ruzicka, Efficacy and safety of a novel mucoadhesive clobetasol patch for treatment of erosive oral lichen planus, J. Oral Pathol. Med. (2021) 0–3.

[20] J.G. Edmans, C. Murdoch, M.E. Santocildes-Romero, P.V. Hatton, H.E. Colley, S. G. Spain, Incorporation of lysozyme into a mucoadhesive electrospun patch for rapid protein delivery to the oral mucosa, Mater. Sci. Eng. C 112 (2020), 110917.

[21] C.A. Schneider, W.S. Rasband, K.W. Eliceiri, NIH image to ImageJ: 25 years of image analysis, Nat. Methods 9 (2012) 671–675.

[22] J. Schindelin, I. Arganda-carreras, E. Frise, V. Kaynig, T. Pietzsch, S. Preibisch, C. Rueden, S. Saalfeld, B. Schmid, J. Tinevez, D.J. White, V. Hartenstein, P. Tomancak, A. Cardona, PBMCs, Nat. Methods 9 (2012) 676–682.

[23] G. Song, Y. Lin, Z. Zhu, H. Zheng, J. Qiao, C. He, H. Wang, Strong fluorescence of poly (N-vinylpyrrolidone) and its oxidized hydrolyzate, Macromol. Rapid Commun. 36 (2015) 278–285.

[24] C. Murdoch, S. Tazzyman, S. Webster, C.E. Lewis, Expression of Tie-2 by human monocytes and their responses to angiopoietin-2, J. Immunol. 178 (2007) 7405–7411.

[25] B. Ollington, H.E. Colley, C. Murdoch, Immunoresponsive tissue-engineered oral mucosal equivalents containing macrophages, Tissue Eng. - Part C Methods 27 (2021) 462–471.

[26] W.R. Gombotz, S.C. Pankey, D. Phan, R. Drager, K. Donaldson, K.P. Antonsen, A. S. Hoffman, H.V. Raff, The stabilization of a human IgM monoclonal antibody with poly(vinylpyrrolidone), Pharm. Res. 11 (1994) 624–632.

[27] D.H. Atha, K.C. Ingham, Mechanism of precipitation of proteins by polyethylene glycols. Analysis in terms of excluded volume, J. Biol. Chem. 256 (1981) 12108–12117.

[28] A.C. Miklos, C. Li, N.G. Sharaf, G.J. Pielak, Volume exclusion and soft interaction effects on protein stability under crowded conditions, Biochemistry 49 (2010) 6984–6991.

[29] M. Gandhi, R. Srikar, A.L. Yarin, C.M. Megaridis, R.A. Gemeinhart, Mechanistic examination of protein release from polymer nanofibers, Mol. Pharm. 6 (2009) 641–647.

[30] U. Angkawinitwong, S. Awwad, P.T. Khaw, S. Brocchini, G.R. Williams, Electrospun formulations of bevacizumab for sustained release in the eye, Acta Biomater. 64 (2017) 126–136.

[31] V. Truong-Le, P.M. Lovalenti, A.M. Abdul-Fattah, Stabilization challenges and formulation strategies associated with oral biologic drug delivery systems, Adv. Drug Deliv. Rev. 93 (2015) 95–108.

[32] N. Simon, C. Sperber, C. Voigtländer, J. Born, D. F. Gilbert, S. Seyferth, G. Lee, B. Kappes and O. Friedrich, Improved stability of polyclonal antibodies: a case study with lyophilization-conserved antibodies raised against epitopes from the malaria parasite plasmodium falciparum, Eur. J. Pharm. Sci., DOI:https://doi.org/10.1016/j.ejps.2019.105086.

[33] D.C. Geraldes, V.L. Beraldo-de-Araújo, B.O.P. Pardo, A. Pessoa Junior, M. A. Stephano, L. de Oliveira-Nascimento, Protein drug delivery: current dosage form profile and formulation strategies, J. Drug Target. 28 (2020) 339–355.

[34] H. Frizzell, T.J. Ohlsen, K.A. Woodrow, Protein-loaded emulsion electrospun fibers optimized for bioactivity retention and pH-controlled release for peroral delivery of biologic therapeutics, Int. J. Pharm. 533 (2017) 99–110.

[35] L.C. Junqueira, J. Carneiro, R.O. Kelly, Basic Histology, Prentice-Hall, London, 1995.

[36] L. Heinemann, Y. Jacques, Oral insulin and buccal insulin: a critical reappraisal, J. Diabetes Sci. Technol. 3 (2009) 568–584.

[37] M.K. Gutniak, H. Larsson, S.J. Heiber, O.T. Juneskans, J.J. Holst, B. Ahrén, Potential therapeutic levels of glucagon-like peptide I achieved in humans by a buccal tablet, Diabetes Care 19 (1996) 843–848.

[38] L. Bierbaumer, U.Y. Schwarze, R. Gruber, W. Neuhaus, Cell culture models of oral mucosal barriers: a review with a focus on applications, culture conditions and barrier properties, Tissue Barriers 6 (2018) 1–42.

[39] M. B. Stie, J. R. Gätke, I. S. Chronakis, J. Jacobsen and H. M. Nielsen, Mucoadhesive Electrospun Nanofiber-Based Hybrid System with Controlled and Unidirectional Release of Desmopressin.

[40] W.M. Saltzman, J.K. Sherwood, D.R. Adams, P. Haller, Long-term vaginal antibody delivery: delivery systems and biodistribution, Biotechnol. Bioeng. 67 (2000) 253–264.

[41] P.Y. Kuo, J.K. Sherwood, W.M. Saltzman, Topical antibody delivery systems produce sustained levels in mucosal tissue and blood, Nat. Biotechnol. 16 (1998) 163–167.

[42] C. Monaco, J. Nanchahal, P. Taylor, M. Feldmann, Anti-TNF therapy: past, present and future, Int. Immunol. 27 (2015) 55–62.

[43] R. K. Jain, Physiological barriers to delivery of monoclonal antibodies and other macromolecules in tumors, Cancer Res.

[44] L.R. Jennings, H.E. Colley, J. Ong, F. Panagakos, J.G. Masters, H.M. Trivedi, C. Murdoch, S. Whawell, Development and characterization of *in vitro* human oral mucosal equivalents derived from immortalized Oral keratinocytes, Tissue Eng. Part C Methods 22 (2016) 1108–1117.

[45] A. Henry, J. Kennedy, G. Fossati, A. Nesbitt, TNF binding by certolizumab pegol, adalimumab, and infliximab-stoichiometry, complex formation, and the biologic effects of complexes, Clin. Immunol. 123 (2007) S169–S170.

[46] R. Lu, J. Zhang, W. Sun, G. Du, G. Zhou, Inflammation-related cytokines in oral lichen planus: an overview, J. Oral Pathol. Med. 44 (2015) 1–14.

[47] J. Mestas, C.C.W. Hughes, Of mice and not men: differences between mouse and human immunology, J. Immunol. 172 (2004) 2731–2738.

[48] K. Moharamzadeh, H. Colley, C. Murdoch, V. Hearnden, W.L. Chai, I.M. Brook, M. H. Thornhill, S. MacNeil, Tissue-engineered oral mucosa, J. Dent. Res. 91 (2012) 642–650.

[49] N.P. Yadev, C. Murdoch, S.P. Saville, M.H. Thornhill, Evaluation of tissue engineered models of the oral mucosa to investigate oral candidiasis, Microb. Pathog. 50 (2011) 278–285.

[50] J.K. Buskermolen, C.M.A. Reijnders, S.W. Spiekstra, T. Steinberg, C.J. Kleverlaan, A.J. Feilzer, A.D. Bakker, S. Gibbs, Development of a full-thickness human gingiva equivalent constructed from immortalized keratinocytes and fibroblasts, Tissue Eng. - Part C Methods 22 (2016) 781–791.

[51] H.E. Colley, V. Hearnden, A.V. Jones, P.H. Weinreb, S.M. Violette, S. MacNeil, M. H. Thornhill, C. Murdoch, Development of tissue-engineered models of oral dysplasia and early invasive oral squamous cell carcinoma, Br. J. Cancer 105 (2011) 1582–1592.

[52] H.E. Colley, P.C. Eves, A. Pinnock, M.H. Thornhill, C. Murdoch, Tissue-engineered oral mucosa to study radiotherapy-induced oral mucositis, Int. J. Radiat. Biol. 89 (2013) 907–914.

[53] T. M. Ferrisse, A. B. de Oliveira, M. P. Palaçon, E. V. Silva, E. M. S. Massucato, L. Y. de Almeida, J. E. Léon and A. Bufalino, The role of CD68+ and CD163+ macrophages in immunopathogenesis of oral lichen planus and oral lichenoid lesions, Immunobiology, https://doi.org/10.1016/j.imbio.2021.152072.

[54] L. Preeti, K.T. Magesh, K. Rajkumar, R. Karthik, Recurrent aphthous stomatitis, J. Oral Maxillofac. Pathol. 15 (2011) 252–256.

[55] J. Fang, C. Wang, C. Shen, J. Shan, X. Wang, L. Liu, Y. Fan, The expression of CXCL10/CXCR3 and effect of the axis on the function of T lymphocyte involved in oral lichen planus, Inflammation 42 (2019) 799–810.

[56] F. Castellino, A.Y. Huang, G. Altan-Bonnet, S. Stoll, C. Scheinecker, R.N. Germain, Chemokines enhance immunity by guiding naive CD8+ T cells to sites of CD4+ T cell-dendritic cell interaction, Nature 440 (2006) 890–895.

[57] T. Suzuki, S.I. Hashimoto, N. Toyoda, S. Nagai, N. Yamazaki, H.Y. Dong, J. Sakai, T. Yamashita, T. Nukiwa, K. Matsushima, Comprehensive gene expression profile of LPS-stimulated human monocytes by SAGE, Blood 96 (2000) 2584–2591.

[58] H. Mühl, C.A. Dinarello, Macrophage inflammatory protein-1 alpha production in lipopolysaccharide-stimulated human adherent blood mononuclear cells is inhibited by the nitric oxide synthase inhibitor N(G)-monomethyl-L-arginine, J. Immunol. 159 (1997) 5063–5069.

[59] J. Li, G.W. Ireland, P.M. Farthing, M.H. Thornhill, Epidermal and oral keratinocytes are induced to produce RANTES and IL-8 by cytokine stimulation, J. Invest. Dermatol. 106 (1996) 661–666.

[60] V. Appay, S.L. Rowland-Jones, RANTES: a versatile and controversial chemokine, Trends Immunol. 22 (2001) 83–87.

[61] M. Contardi, M. Summa, P. Picone, O.R. Brancato, M. Di Carlo, R. Bertorelli, A. Athanassiou, Evaluation of a multifunctional polyvinylpyrrolidone/hyaluronic acid-based bilayer film patch with anti-inflammatory properties as an enhancer of the wound healing process, Pharmaceutics 14 (2022) 483.

[62] V. Dennis, S. Singh Yilma, S. Dixit, Anti-inflammatory effects of silver-polyvinyl pyrrolidone (Ag-PVP) nanoparticles in mouse macrophages infected with live chlamydia trachomatis, Int. J. Nanomedicine 2421 (2013).

[63] G. Burgess, M. Boyce, M. Jones, L. Larsson, M.J. Main, F. Morgan, P. Phillips, A. Scrimgeour, F. Strimenopoulou, P. Vajjah, M. Zamacona, R. Palframan, Randomized study of the safety and pharmacodynamics of inhaled interleukin-13 monoclonal antibody fragment VR942, EBioMedicine 35 (2018) 67–75.